A Deep Learning Framework for Generation and Analysis of Driving Scenario Trajectories

SN Computer Science (2023) 4:251
https://doi.org/10.1007/s42979-023-01714-3

ORIGINAL RESEARCH

A Deep Learning Framework for Generation and Analysis of Driving Scenario Trajectories

Andreas Demetriou[1] · Henrik Alfsvåg[1] · Sadegh Rahrovani[2] · Morteza Haghir Chehreghani[1]

Received: 7 July 2022 / Accepted: 28 January 2023

Abstract
We propose a unified deep learning framework for the generation and analysis of driving scenario trajectories, and validate its effectiveness in a principled way. To model and generate scenarios of trajectories with different lengths, we develop two approaches. First, we adapt the Recurrent Conditional Generative Adversarial Networks (RC-GAN) by conditioning on the length of the trajectories. This provides us the flexibility to generate variable-length driving trajectories, a desirable feature for scenario test case generation in the verification of autonomous driving. Second, we develop an architecture based on Recurrent Autoencoder with GANs to obviate the variable length issue, wherein we train a GAN to learn/generate the latent representations of original trajectories. In this approach, we train an integrated feed-forward neural network to estimate the length of the trajectories to be able to bring them back from the latent space representation. In addition to trajectory generation, we employ the trained autoencoder as a feature extractor, for the purpose of clustering and anomaly detection, to obtain further insights into the collected scenario dataset. We experimentally investigate the performance of the proposed framework on real-world scenario trajectories obtained from in-field data collection.

Keywords Generative Adversarial Networks (GANs) · Time series analysis · Autonomous drive safety verification · Clustering · Outlier detection

Introduction

The future of transportation is tightly connected to Autonomous Driving (AD). While a lot of progress has been made in recent years in these areas, there are still obstacles to overcome. One of the most critical issues is the safety verification of AD. To assess with confidence the safety of AD, statistical analyses have shown that fully autonomous vehicles would have to be driven for hundreds of millions of kilometers [21]. This is not feasible, particularly in cases when we need to assess different system design proposals or in case of system changes, since the same amount of distance needs to be driven again by the AD vehicle for the verification sign-off. Thus, a data-driven scenario-based verification approach that shifts performing tests in the fields to a virtual environment provides a systematic approach to tackle safety verification. This approach requires a scenario database to be created by extracting driving scenarios (e.g. cut-in, overtaking, etc.) that the AD vehicle is exposed to in naturalistic driving situations. Scenarios are obtained through time series (sequence of the ego-vehicle states and the surrounding objects) which in turn are the processed data collected by sensors of the AD vehicle. Once such a scenario database is developed, it can be used for test case generation and verification of the AD functionality in a virtual environment [22]. Note that, scenario extraction can, in general, be addressed with two approaches: an explicit rule-based approach [42] (that requires expert domain knowledge) and a (machine learning based) clustering approach [26, 33, 37, 38], where they can complement each other. Figure 1 illustrates the high-level overview of the full process from the raw logged data to the scenario database with a sufficient number of scenarios for verification.

Andreas Demetriou, Henrik Alfsvåg, Sadegh Rahrovani and Morteza Haghir Chehreghani have contributed equally to this work.

✉ Morteza Haghir Chehreghani
morteza.chehreghani@gmail.com

[1] Department of Computer Science and Engineering, Chalmers University of Technology, Gothenburg, Sweden

[2] Autonomous Drive Department in Volvo Cars, Gothenburg, Sweden

Published online: 04 March 2023

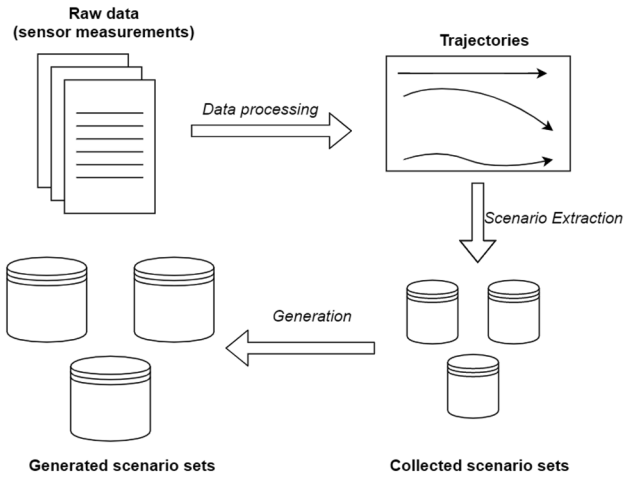

Fig. 1 The full workflow from raw data to scenario database

However, several challenges should be addressed to create a reliable scenario database. First, a huge amount of data is still needed to be collected and processed to build such a scenario database. In particular, the existing data might be imbalanced or insufficient. Second, to assure safety in vehicles, AD functionality needs to pass safety tests not only based on "real" scenarios (also called test cases) collected from field driving tests, but also based on many perturbed (similar) trajectories that might have not been collected in real driving data collection. To address these issues, building generative models (by mimicking the variation available in the collected scenario data) to create realistic synthetic scenarios is a main focus of this work.

Thereby, we propose a unified deep learning framework for generation and analysis of driving scenario trajectories, and validate its effectiveness in a principled way. We investigate the performance of different variants of Generative Adversarial Networks (GANs) [13] for generating driving trajectories. GANs have shown promising results in several tasks related to the generation of synthetic data. In this paper, since the data are sequential, we employ recurrent architectures to extract the sequential nature of data. The first approach consists of a recurrent GAN (without an autoencoder). We adapt the Recurrent Conditional Generative Adversarial Networks (RC-GAN) by conditioning on the length of the trajectories. This provides us the flexibility to generate variable-length driving trajectories, a desirable feature for scenario test case generation in AD verification. The second approach consists of a recurrent autoencoder and a GAN for learning/generating latent-space representations of trajectories of different lengths. In this approach, it is essential to know the length of the trajectories to bring them back from the latent space representation. We overcome this issue by training an integrated feed-forward neural network to estimate the lengths based on the latent space representations.

At the same time, the recurrent autoencoder can be used as a feature extractor. Thus, we analyze such latent space features in the context of exploratory data analysis to obtain further insights into the collected scenario set via clustering and anomaly detection. As mentioned earlier, clustering can be useful for scenario extraction, as an alternative solution to explicit rule-based methods that might be subject to misspecification. Clustering can also provide an effective tool for data visualization and exploration. We demonstrate the performance of the framework on real-world in-field scenario trajectories collected by Volvo Cars Corporation (VCC).

This work is an extension of our publication in [7]. The extension includes different aspects such as (i) further elaboration of the methods on trajectory generation using GANs, (ii) a clustering method consistent with the proposed deep learning framework, in particular with the respective latent representation, (iii) an outlier detection mechanism of the trajectories based on the latent space representation using the developed recurrent autoencoder, (iv) discussion on the applicability of the proposed clustering and outlier detection mechanisms for Autonomous Driving applications, and (v) novel experimental studies and investigations, in particular for the clustering and outlier detection components.

Background

Problem Description

We are provided with the data collected by Volvo Cars Corporation. This dataset consists of information about the ego vehicle and its surroundings such as detected objects, road conditions, etc. We focus on generating realistic scenario trajectories, in particular, the cut-in trajectories for a specific tracked vehicle, and their analysis in the context of exploratory data analysis. To describe a trajectory, we consider two features: the relative lateral and longitude positions of the vehicle with respect to the ego vehicle.

To generate and analyze trajectories, our framework performs the following steps.

- Extract scenarios from the logged data, which is done with explicit rules defined by an expert. Note that all surrounding/target cars in the field of view (of the ego car), and the lane marking signals are available. So the rule-based scenario functions work based on this information and they assign a start time stamp and end timestamp to a scenario (e.g., start the cut-in scenario a couple of seconds before the target car passes the lane marking and enters the ego car's lane, and stop cut-in after the

target car becomes the lead car in front of the ego car). This will be discussed more in the next section, Scenario Extraction.
- Build the generative models for synthesizing/generating trajectories similar to the ones collected from the in-field test.
- Evaluate the obtained results and compare the generated trajectories versus the real ones. This step is done by visual inspection and the metrics that will be introduced.

Besides the explicit rule-based approach for scenario extraction, a clustering method can be used as well. Clustering has some advantages. Firstly, it enables one to detect scenarios that lie on the border of two scenario classes and thus finds more complex driving patterns/scenarios. Second, explicit rules could miss outliers. Moreover, explicit rules require expert domain knowledge and a hard threshold to define scenarios, which is nontrivial to formulate and calibrate when the dimensionality of data increases. Thus, clustering, when used in combination with an explicit rule-based approach, provides exploratory insights from the data and is suitable w.r.t. scalability. Also, the labels provided by the explicit rule-based approach can be verified by the clustering-based approach for consistency, where the false positive/negative cases can be investigated further by camera sensors video check. Calibration of scenario definition threshold could be done afterwards, when these valuable misclassified labels have been investigated. This consistency check between the two approaches can accelerate the label verification process considerably since only a limited number of video checking might be required.

Related Work

Generation

One approach to generate driving trajectories is based on simulations of physical models, including the vehicle dynamics and driver model. This is a promising approach, but it needs to be used in combination with other solutions, as validating those simulation models is as challenging as the verification of the AD problem. Also, the simulation of high-fidelity models can be computationally demanding w.r.t. computational and storage resources.

GANs [13] are the most popular paradigms for synthetic data generation in the context of modern deep neural networks. They have been employed and developed in several applications such as image processing, computer vision, text generation, natural language processing and translation [6, 20, 23, 25, 41].

A related work has been developed based on generating errors for the sensors' measurements using recurrent conditional GANs [1]. This method can be used to make simulated data look more realistic. The study in [24] considers the rather similar problem of maneuver modeling with InfoGAN and β-VAE. These generative models show satisfactory results. However, the data in this work are collected by a drone which we consider to be a limitation. In [8] presents 'Multi-vehicle Trajectory Generator' (MTG) that is an improved version of β-VAE with recurrent networks. Moreover, it shows that the proposed MTG produces more stable results than InfoGAN or β-VAE.

Clustering

Several methods have been proposed for clustering based on time series and trajectory analysis [2, 27], in particular for vehicle trajectories clustering [19, 26, 33, 37]. Some methods use Hidden Markov Models (HMM) to deal with the sequential aspects of time series and trajectories, which are usually computationally expensive [29, 36, 39]. Recent work uses Mixture of Hidden Markov Models (MHMM) that has shown promising results [33]. An advantage of HMM is simplicity and interpretation.

TimeNet, proposed in [32], is a multilayered recurrent neural network for feature extraction from time series. The authors demonstrate the performance of TimeNet on tasks such as classification and clustering where they compute an embedding based on t-SNE [31]. Embedding the time-series has been also studied in [35], where the proposed method, called m-TSNE, uses Dynamic Time Wrapping (DTW) [12] as a metric between multidimensional time series embedded by t-SNE. The work in [19] develops a trajectory clustering method based on embedding temporal relations via DTW and deep learning, and then extracting the transitive relations via minimax distances [15, 17]. Finally, it is notable that clustering sequential data clustering is beyond trajectory analysis and has been studied for example for tree-structured sequences in [4].

Driving Scenario Data Source

Scenario Extraction

The objects' trajectories are extracted from the raw data (sensor measurements) and fused sensor data, which are mounted on the ego car. Thus, the reference/coordinate system is the ego car. Since it is a moving reference, then all the measured signals (i.e., the position of the surrounding cars/objects) are relative with respect to the ego car. These trajectories can vary in length from 1 s up to 1 h. The length depends on how long the object is tracked by the ego-vehicle in the field of view (FoV). The specific scenarios of high interest are cut-ins. There are many different definitions of what constitutes a cut-in. We define them as vehicles that

approach the ego vehicle from the left lane and then overtake the ego vehicle by switching to its lane. Therefore, the cut-ins vary in aggressiveness. More specifically, our definition of a cut-in also requires the vehicle to stay in front of the ego vehicle for at least 2 s. An example of the extracted trajectory is illustrated in Fig. 2. Note that plotting trajectories as a line as shown in Fig. 2a has the disadvantage of *eliminating* the time component as compared to Fig. 2b. However, we find this way more expressive, as otherwise, it becomes extremely cluttered when multiple trajectories overlap.

On the Issue of Variable-Length Trajectories

One of the main issues in analyzing the trajectories is the variable-length input/output, which in our case varies from 30 to 70 time frames (from 3 to 7 s given the sampling rate of 10Hz). One solution is to train the model with padding. To apply padding, a pad token has to be defined. For instance, in natural language processing, it is common to employ word embedding and then to use zero vectors as a pad token [5]. Unfortunately, it is not a trivial task to define a pad token in case of real coordinates as any pair of real numbers is a realistic point in space. A possible solution is to pad sequences with the last point. However, it does not seem a feasible approach in our case due to the high variation in length (the shortest sequence after padding will contain more than 50% pad tokens). These paddings not only may affect the distribution of the generated samples significantly, but also might call for post-processing of the samples. For example, if the last n points are the same they should be considered as padding and erased. This yields an intrinsic problem as the definition of 'being the same' is non-obvious in particular when some noise is added during the generation. Such problems can be avoided by feeding the sequences to the model one-by-one. However, this approach will greatly decline the performance.

Thus, in the proposed approach, we group the sequences with the same length together to form a batch. In this way, we train a model for the whole data but with different batches, where each batch represents a specific trajectory length. For example, assume trajectories of the following lengths (1–30 denotes that the trajectory number 1 has length 30): 1–30, 2–32, 3–32, 4–32, 5–34, 6–34, 7–34, and 8–34. Then, the following batches are formed: $\{1\}, \{2, 3, 4\}, \{5, 6, 7, 8\}$. If one propagation through the model takes 1 unit of time, then training the model with these batches would take 3 units of time, compared to 8 units of time with the one-by-one trajectory processing approach. The next steps depend on the architecture of the generative model, to be studied later.

Trajectory Generation Framework

To model and generate scenarios of trajectories with different lengths, we develop and propose two methods: (i) An architecture based on combined Recurrent Autoencoder with GANs, where to obviate the variable length issue, the GAN is trained to learn/generate the hidden representation of original trajectories, instead of the original sequential data. (ii) A Recurrent Conditional GANs (RC-GAN) architecture that

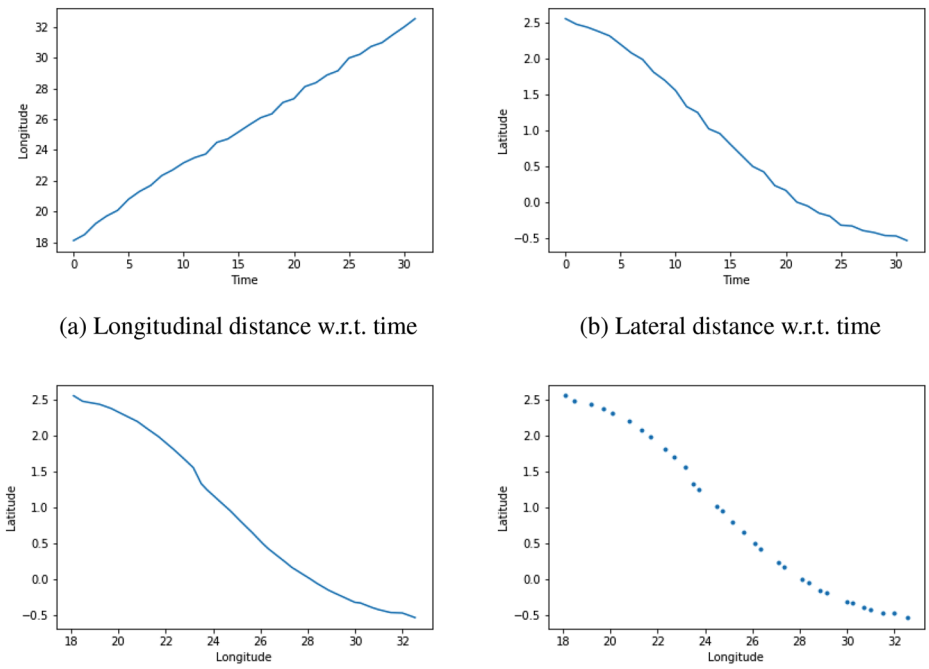

(a) Longitudinal distance w.r.t. time

(b) Lateral distance w.r.t. time

(c) Lateral distance w.r.t. longitudinal distance

(d) Lateral distance w.r.t. longitudinal distance

Fig. 2 The extracted cut-in in different forms: (**a**) and (**b**) show the longitudinal and lateral distances w.r.t. time, and (**c**) and (**d**) illustrate the lateral distance w.r.t. longitudinal distance

enables us to generate driving sequences with pre-specified length, which is a desirable and useful feature when generating test cases for AD verification. In the following, we explain on each of the two methods in detail.

The Architecture: Autoencoder with GANs (AE-GAN)

This solution is based on the architecture proposed for text generation in [9]. It consists of an autoencoder for time series as shown in Fig. 3 and GAN for latent space representation and data generation.

We adapt and extend this architecture to deal with variable-length input/output. It is essential to know the length of the sequence to bring it back from the latent-space representation. During the autoencoder training, the length is known from the input, but for the artificial latent-space vectors generated by GANs it is necessary to estimate the length of the trajectory. We address this issue by training a separate feed-forward neural network to estimate the lengths based on the latent space representation.

Hence, once the autoencoder is trained, all trajectories are encoded to the latent space using the encoder. During this process, the length of each trajectory is stored. Thus, two sets are created: X: the set of latent representations, and Y: the set of the lengths for each trajectory. With these sets, the task of length estimation from latent space can be considered a supervised regression task which can be solved using a feed-forward neural network, as shown in Fig. 4.

At this stage, GANs are used to generate new latent-space representations. Even though it seems reasonable to implement both the generator and the discriminator as standard fully-connected neural networks, we will also investigate the ResNet model [18] to mitigate the problems related to gradient instability, similar to the work in [9]. To train GANs, we consider two alternatives: the standard GAN and the Wasserstein GAN with Gradient Penalty (WGAN-GP) [14].

As the latent-space representation is generated, it is used as an input to the decoder. To determine how many times to apply LSTM cell, we employ the aforementioned neural network in Fig. 4.

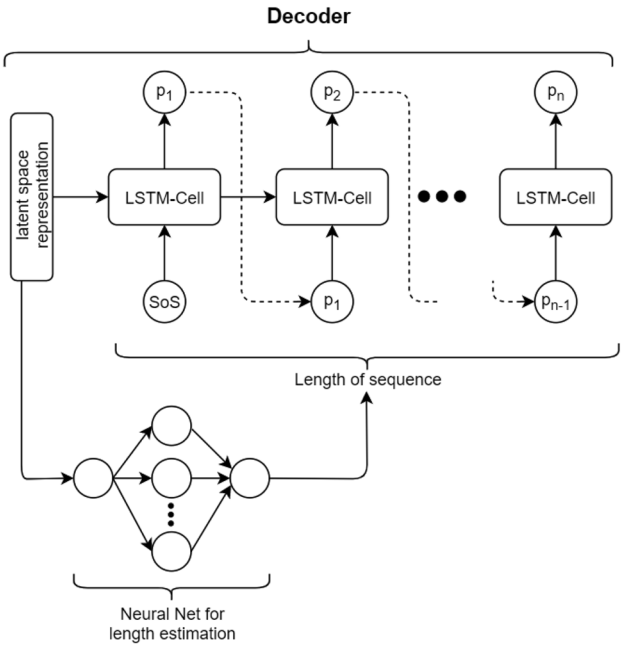

Fig. 4 Structure of the decoder part of the autoencoder combined with a Length Estimator to reconstruct trajectories from latent space representation

The Architecture: Recurrent Conditional GANs (RC-GAN)

Recurrent GANs (RecGANs) have shown promising results for generating time series in several applications such as music generation [34], real-valued medical data [10] and sensor error modeling [1]. In this paper, we adapt them for our task as follows. Both the generator and discriminator are Recurrent NNs (RNNs) based on LSTM cells. For the discriminator, we choose a bidirectional architecture. At every time step i, each LSTM cell in the generator receives a random input (i.e., z drawn from $\mathcal{N}(0,1)$) and the hidden vector from the previous cell, to generate p_i. For the first cell, the previous hidden vector is initialized to 0. The sequence $p_1 ... p_n$ forms the final trajectory, that is passed to the discriminator. Then, the discriminator computes a sequence of

Fig. 3 Schematic structure of recurrent autoencoder

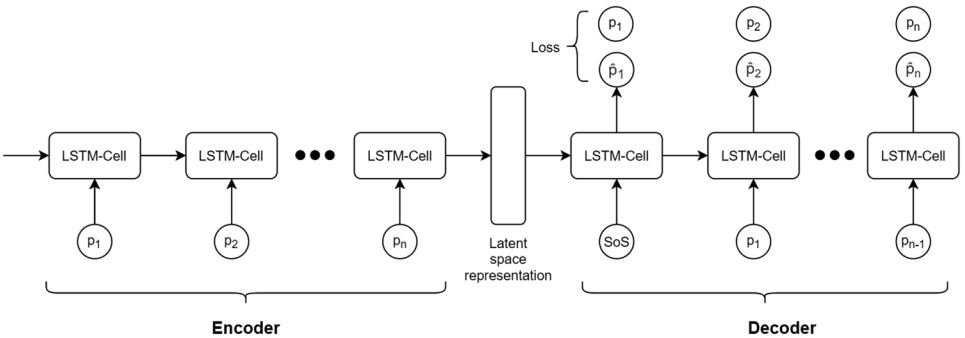

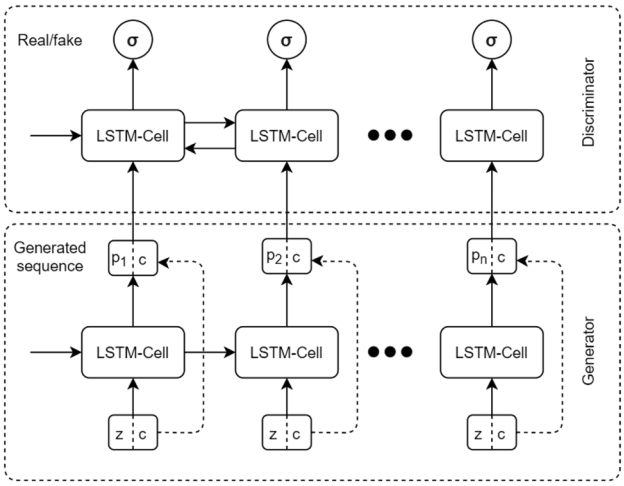

Fig. 5 The schematic structure of RC-GAN

probabilities (σ in Fig. 5) identifying whether the trajectory is real or fake. The ground truth is a sequence of ones for the real trajectories and zeros for the fakes. RecGANs can also be conditional. With Recurrent Conditional GANs (RCGANs), the condition might be passed as an input into each cell for both the discriminator and the generator. As shown in [10], the condition can be simply concatenated to the generator's input and output (Fig. 5). This allows the discriminator to distinguish between reals and fakes w.r.t. to condition, that in turn forces the generator to produce samples w.r.t condition. To adapt this architecture to our task, we use the length of a trajectory as a condition and attach it to the input.

Evaluation

An important and challenging task is to choose proper metrics to evaluate the quality of the generated trajectories [30]. One might first evaluate the results via visualization to see whether they do make sense. However, as the results improve it becomes harder to determine precisely how good they are. Thus, it is important to consider quantitative evaluation metrics as well, such that one can objectively quantify the similarity of the generated trajectories with the original ones.

Table 1 Pairwise distances between trajectories from two sets, here *tr* stands for the trajectory

	Set 1			
	tr_1	tr_2	.	tr_n
Set 2				
tr'_1	$\text{dist}(tr'_1, tr_1)$	$\text{dist}(tr'_1, tr_2)$	.	$\text{dist}(tr'_1, tr_n)$
tr'_2	$\text{dist}(tr'_2, tr_1)$	$\text{dist}(tr'_2, tr_2)$	.	$\text{dist}(tr'_2, tr_n)$
.	.	.	$\ddots$	.
tr'_n	$\text{dist}(tr'_n, tr_1)$	$\text{dist}(tr'_n, tr_2)$	.	$\text{dist}(tr'_n, tr_n)$

One commonly used method to measure similarities between time series is Dynamic Time Warping (DTW). Thus, to compare sets of time series, we build a matrix of pairwise DTW distances between the samples from the two sets as shown in Table 1. Such a matrix can be used to find the most similar samples from the two investigated sets. In addition, we analyze this pairwise matrix using the following two metrics. In the following, we describe two methods for the analysis of results based on matching the time series.

Matching + Coverage

We match each sample from the generated set (called GS_M with M samples) with the closest sample from the real set (called RS_N with N samples). The matching criterion is defined by

$$\text{matching} = \frac{\sum_i^M \min_j (\text{dist}(GS_i, RS_j))}{M}. \tag{1}$$

Even if reasonable results are achieved with this metric, it does not necessarily indicate that the model performs well, since many generated samples can be 'mapped' to the same real sample. In this case, the coverage of the model is low. Thus, we also measure a coverage metric as follows.

$$\text{coverage} = \frac{|\text{argmin}_j(\text{dist}(GS_i, RS_j)), \forall i = \overline{1, M}|}{N}. \tag{2}$$

However, even the combination of these two metrics still has shortcomings. For instance, if there are two (or more) similar samples in the real set and many generated samples are 'mapped' to one of the real samples, then the coverage decreases. However, this does not mean that the model performs poorly. Since the sets are very diverse, we consider GS_M and RS_N with $M > N$. In our experiments, we use $M = 4 * N$.

One-to-One Matching with Hungarian Method

The Hungarian algorithm is a matching method for one-to-one matching. Applying it to Table 1 yields mapping each sample from the generated set to exactly one sample from the real set. This mapping ensures that the sum of distances of the paired samples is minimal. The main disadvantage of this method is the sample distributions in the real and generated sets may not be identical. For example, the last 10% of the matched samples can be outliers that are from irrelevant parts of the distribution.

Once the aforementioned metrics are defined it is still an open question which ground truth should be used as a reference to compare the results with. To address this question,

we split the real dataset into different subsets and apply these metrics among the different subsets. We use the results as a baseline when analyzing the trajectories obtained from the generation models.

Exploratory Analysis of Latent Space Representations

GANs provide an unsupervised learning approach to generate samples consistent with a given set of real trajectories. In the following, we investigate other unsupervised learning methods in the context of clustering and outlier detection, to obtain exploratory insights from the driving trajectories of the surrounding objects, collected by sensors of the ego car. In addition, as mentioned before, these methods can be useful for the safety verification of AD. Consistent with the proposed GAN architectures, our clustering and outlier analysis mechanisms are also performed based on the latest space representation obtained from training the autoencoder. This helps us to benefit from the representation that encodes the temporal aspects of the trajectories and simplifies the process. We note that the solution from the latent space representations can be transferred to the original trajectories, to provide a solution in the original data space.

Performing for example the clustering on original trajectories might require methods such as DTW to model the temporal aspects first. Then, we may apply a high-dimensional data visualization and grouping method such as t-SNE [31]. The method proposed in [35] and called m-TSNE applies t-SNE to DTW-based (dis)similarity matrix. However, it is computationally very expensive, when working with a large number of scenario trajectories. In the case of n trajectories of length m, it needs to calculate n^2 pairwise distances and each distance is computed with DTW that runs in $O(m^2)$. Thus, the overall performance is $O(n^2m^2)$. In our setup, we have relatively long trajectories (50 time step on average) and relatively a large number of them. Therefore, we employ the already trained autoencoder which encodes the temporal dependencies properly. We assume that clustering and outlier detection at latent space is an easier task with reasonable computational costs.

Clustering on Latent Space with Autoencoder

Here, we study clustering the latent space representation of trajectories, obtained by recurrent autoencoder. For this purpose, we extract three types of scenarios: cut-in, left drive-by and right drive-by, as shown in Fig. 6.

Drive-by occurs much more frequently. Thus, the cut-in set contains fewer trajectories compared to the drive-by set. To address this issue, we do oversampling for the cut-in set and undersampling for the drive-by sets. Then, we train the autoencoder and encode all the trajectories. This step converts all trajectories to fixed-size vectors. Even though the resultant latent space representations are fixed-size, they are still high dimensional. Thus, it might be challenging to cluster them directly with distance-based algorithms such as K-means or DBSCAN. Therefore, we reduce the dimensionality with methods such as Principal Component Analysis (PCA) and t-SNE. Finally, we apply the clustering method (e.g., DBSCAN [11]) and analyze the results. The procedure is described in Fig. 7, where the encoder part is the same for all trajectories and p_i represents lateral and longitudinal positions in our case. In this way, each trajectory is mapped to a two-dimensional representation.

Outlier Detection with Autoencoder

Being able to detect anomaly driving patterns and outliers among scenario trajectories is very valuable in different aspects in particular when the data is imbalanced. First, it can be used to assess the quality of the original data and to find possible sensor reading anomalies/errors. A more detailed investigation can be then performed afterwards, by checking the camera videos and LIDAR sensor reads, to gain more insights about the detected anomalies. Second, it can be used to find the minority sub-groups in the data. For example, aggressive driving of the surrounding vehicles w.r.t. ego vehicle is an important test case for verification of AD functionality. Having this information about anomalies can also improve the quality of the generation process by treating them differently. Third, it is often important to determine if a set of data is homogeneous and balanced before any statistical technique is applied. Finally, this information can help us to re-calibrate our explicit rule-based cut-in finder functions. These functions, which usually are defined based on a hard threshold for a scenario, might perform poorly on anomalies.

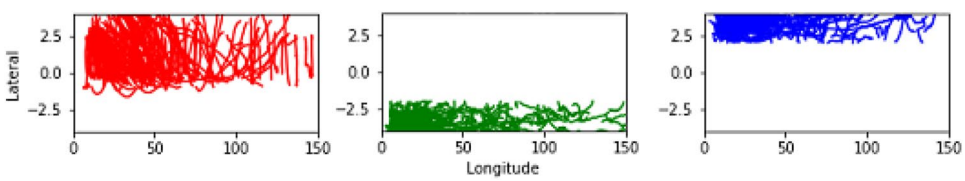

Fig. 6 Three types of explicit-rule extracted trajectories: cut-ins, right- and left drive-by

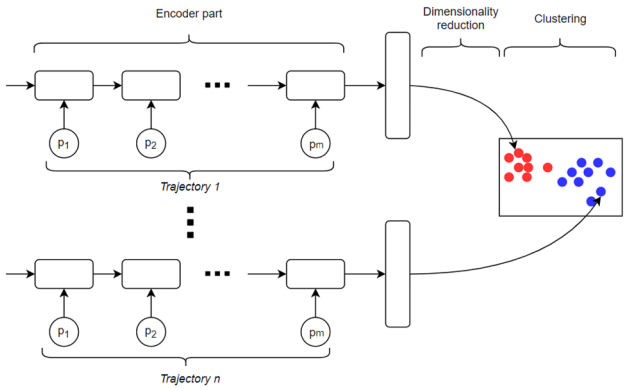

Fig. 7 Clustering process with AE

In the following, we describe a method to detect and analyze outliers using the trained autoencoder. We assume a high reconstruction loss in the autoencoder implies some anomaly in the respective trajectory, i.e., the sample is an outlier. We may define a threshold for the loss and consider all the trajectories that yield a higher reconstruction loss than the threshold as outliers. However, choosing a hard threshed might be nontrivial. On the other, a hard assignment might not be very robust. Therefore, we follow a 'soft' approach instead, where we compute the probability of a trajectory (s_i) being an outlier.

$$p(s_i \text{ is outlier}) = \frac{\exp(l(s_i))}{\exp(l(s^*))}, \tag{3}$$

where s^* corresponds to the trajectory with maximal reconstruction loss. We note that instead of normalization by $\exp(l(s^*))$, one may use any other normalization which might makes sense depending on the context.

Experimental Results

In this section, we investigate the different aspects of the proposed methods on real-world data and scenarios.

Figure 8a shows 100 real trajectories wherein a cut-in occurs. It is clear that the distribution is not even and uniform. There are a lot more samples in the 20-60 ms longitudinal region while only a few are seen past 100 ms. Another observation is that the majority of the trajectories have a trend to increase in the longitudinal distance through time. However, there are several samples for which the longitudinal distance decreases instead. This can be interpreted as the cut-ins wherein the tracked vehicle accelerates or decelerates respectively. It seems worth checking if the proposed models capture these different trends and outliers.

Autoencoder

We start with examining the results from the autoencoder. Figure 8 illustrates the real and reconstructed trajectories. The main difference between them is the smoothness of the reconstructed ones which is a typical and expected property of an autoencoder.

We perform two experiments: the first experiment with the trajectories from 3 to 5 s, and the second experiment with the trajectories from 3 to 7 s. In both cases, a two-layer LSTM cell is used. The loss values with respect to different sizes of hidden states are shown in Table 2. For the first experiment, a hidden state of size 32 is sufficient and produces meaningful results from a visual inspection point of view. However, for the second experiment, we choose the size of the hidden state to be 64 as it decreases the loss drastically. Note that close loss values for trajectories with different lengths does not necessarily imply the same performance for the autoencoder, since the mean is calculated with respect to a different number of samples.

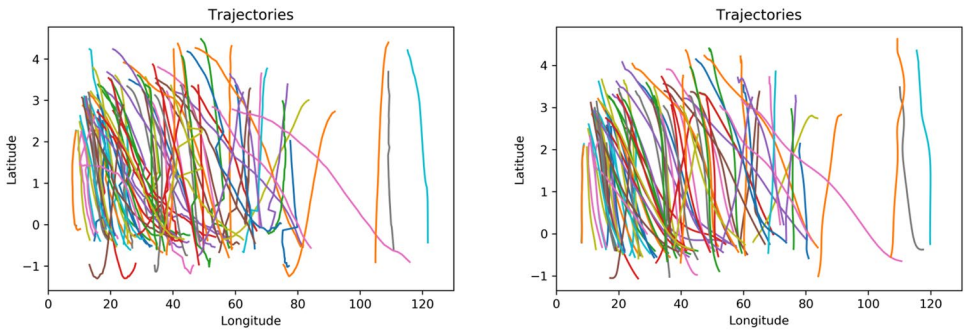

(a) Real Trajectories (b) Reconstructed Trajectories

Fig. 8 Comparison of 100 real trajectories in (**a**), and their reconstruction by autoencoder in (**b**)

Table 2 Comparison between different sizes of hidden state (hs) for two sets consisting of trajectories between 3 to 5 s (I) and 3 to 7 s (II)

Size of hs	Val.Loss I	Train Loss I	Val.Loss II	Train Loss II
32	0.0633	0.0652	0.0648	0.0637
64	0.0619	0.0620	0.0469	0.0469
128	0.0601	0.0610	0.0451	0.0471

Generative Models: AE-GAN & RC-GAN

Figures 9 and 10 illustrate the trajectories generated respectively with RC-GAN and AE-GAN. Obviously, both models capture the trends of the data. However, some of the generated trajectories can be distinguished from the real ones. The samples from RC-GAN are noisier compared to the real ones, while samples generated with AE-GAN are more smooth. From a visual inspection, both models seem to capture the distribution of the trajectories. Similar to the real dataset, there are more trajectories generated close to the ego-vehicle and less further away. Both models also generate accelerating and decelerating cut-ins.

Our proposed RC-GAN is conditioned on the length of the trajectory. It is therefore possible to generate trajectories with a pre-specified length. This condition works as expected. As it can be seen in Fig. 9, all trajectories end up in region 0 (from a lateral perspective), which means they are complete cut-ins. For example, there are no trajectories that are just truncated halfway after 3 s.

With AE-GAN, we start our experiments for trajectories from 3 to 5 s with fully-connected neural networks and original GANs. The results of this experiment are illustrated in Fig. 10a. Unfortunately, this setting does not produce meaningful results for the 3 to 7 s trajectories. Thus, we experiment with the WGAN-GP and ResNet architecture for the generator and the discriminator. The ResNet architecture does not introduce any great improvement. However, WGAN-GP allows us to generate trajectories from 3 to 7 s as shown in Fig. 10b. Figure 11 illustrates the trajectories with minimal DTW distances from RC-GAN and AE-GAN.

Quantitative Comparisons

We first apply the proposed metrics to the real set to obtain a baseline. Each experiment is done 5 times and the average score together with the maximum and minimum scores are reported in Tables 3 and 4 for the first and second metrics, respectively. Note that the experiments with RC-GAN and AE-WGAN-GP are performed for 3 to 7 s trajectories while the results with AE-GAN are only for 3 to 5 s trajectories.

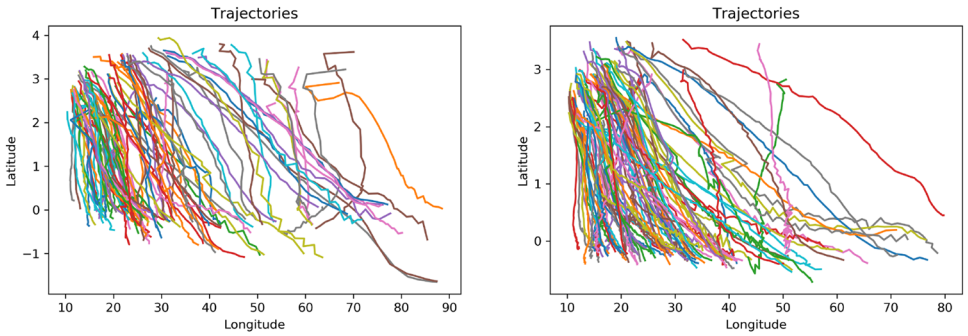

(a) Length from 3 to 4 seconds (b) Length from 6 to 7 seconds

Fig. 9 The trajectories generated with RC-GANs. (**a**): Trajectories of length 3 to 4 seconds, and (**b**): trajectories of length 6 to 7 seconds

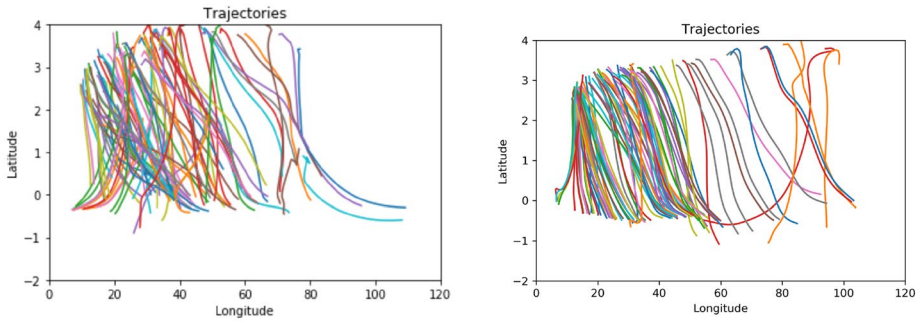

(a) Example of 100 trajectories from 3 to 5 seconds generated with AE-GAN (b) Example of 100 trajectories from 3 to 7 seconds generated with AE-WGAN-GP

Fig. 10 The trajectories generated with AE-GAN and AE-WGAN-GP. (**a**): Trajectories of length 3 to 5 seconds, and (**b**): trajectories of length 3 to 7 seconds

Based on the results of the *Matching+Coverage* metric in Table 3, RC-GAN yields the highest coverage and the lowest matching error among the generated sets. The matching metric for RC-GAN is even lower than the real set which can be explained by a lower coverage: calculating the average for about 60% of the best matched samples in the real set produces a lower score. On the other hand, as discussed in Figs. 9 and 10, the AE-WGAN-GP trajectories are significantly smoother compared to the RC-GAN trajectories. Since the performance of AE-WGAN-GP is still close to the real sets in particular w.r.t. the *Matching* metric, thus it might be preferred in practice.

The results for the second metric that is based on one-to-one matching (i.e., the Hungarian method) are shown in Table 4. The best result belongs to AE-WGAN-GP which is 229.91. It is about three times higher than the result of the real set. However, such behavior is expected due to an uneven distribution of trajectories. To obtain more useful insights from the one-to-one matching, the distances between the matched samples are plotted in Fig. 12. We can

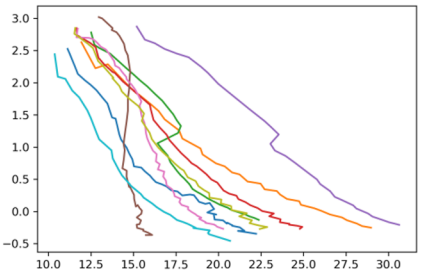

(a) Generated trajectories with RC-GAN.

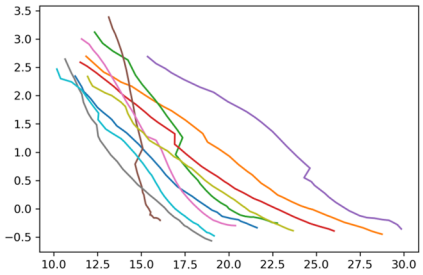

(b) Real trajectories closest to the trajectories presented in (a).

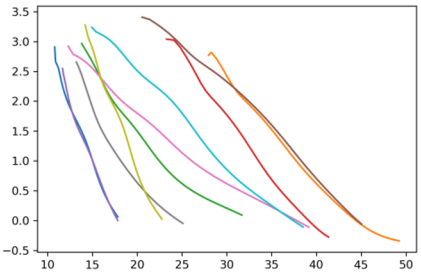

(c) Generated trajectories with AE-GAN.

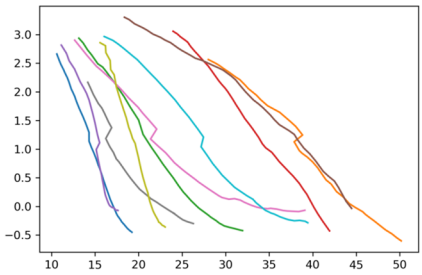

(d) Real trajectories closest to the trajectories presented in (c).

Fig. 11 Illustration of 10 closest samples between generated and real sets. (**a**) shows the generated trajectories with RC-GAN, and the respective closest real trajectories are visualized in (**b**). (**c**) shows the generated trajectories with AE-GAN, and the respective closest real trajectories are illustrated in (**d**)

Table 3 The results for Matching and Coverage metric. Min, Max and Average are computed from 5 experiments

Set	Matching			Coverage		
	Min	Max	Average	Min	Max	Average
Real Set (Baseline)	39.78	45.46	43.28	0.85	0.89	0.875
RC-GAN	29.08	31.93	30.37	0.63	0.68	0.66
AE-GAN	48.85	56.13	53.31	0.39	0.45	0.42
AE-WGAN-GP	39.04	52.65	44.70	0.54	0.59	0.56

Table 4 The results for Hungarian distance. Min, Max and Average are computed from 5 experiments

Set	Hungarian			Hungarian (75%)		
	Min	Max	Average	Min	Max	Average
Real Set (Baseline)	62.01	84.58	75.2	29.84	40.14	36.10
RC-GAN	330.38	500.66	430.33	121.14	151.83	138.56
AE-GAN	330.3	424.59	358.69	121.94	141.74	130.02
AE-WGAN-GP	159.15	284.36	229.91	63.47	102.68	79.32

clearly see similar behavior between the generated and real sets. The scale of these graphs is different, and the matched distances for generated sets explode more compared to the real set. We assume this behavior is a combination of two factors: the dissimilar distribution of trajectories and some generated samples that are far from being realistic. From Fig. 12 it is observed that none of the plots explodes until 150 out of 200 samples. Thus, we also compute an average of the matched distances for only the first 75% of samples, as shown in Table 4. According to these results, the generated samples (in particular by AE-WGAN-GP) are more consistent with the real trajectories.

Clustering

In the following, we investigate clustering and in particular the DBSCAN method on latent space representations. As mentioned before, to handle the high dimensionality issues, DBSCAN [11] is used in combination with dimensionality reduction techniques to reduce the number of dimensions: PCA, SVD and t-SNE. Figure 13 shows the results of different methods in two dimensions. We observe that neither PCA nor SVD transform the data such that it can be clustered properly, i.e., the clusters have overlaps. PCA performs slightly better than SVD, thus we skip SVD. Unlike PCA and SVD, t-SNE provides a non-overlapping and well-separated embedding. With PCA and SVD, we obtain a diagonal matrix Σ with singular values and based on them, it is possible to calculate a percentage of variance introduced by each component. This information can help to find an optimal number of principal components to capture enough information from the original data to distinguish clusters while at the same time avoid the curse of dimensionality.

According to Fig. 13, we find the embedding produced by t-SNE to be the most promising choice to perform clustering. The results of DBSCAN with $\epsilon = 9$ and $minNeighbors = 25$ are shown in Fig. 14a, where five clusters are obtained. Fine-tuning the parameters of DBSCAN, especially, setting $\epsilon = 9.6$ yields a clustering exactly equivalent to the ground-truth solution. Whereas for a wide range of parameters we obtain the five clusters. These five clusters are consistent with the three ground-truth clusters, i.e., none of them is included in more than one ground-truth clusters. This implies that our solution provides a finer and more detailed representation of the data. It is worth mentioning that the labels we obtain from explicit rule-based approach might not describe the real clusters at a sufficient level, i.e., there might exist finer clusters, especially when dealing with complex scenarios. One may use a hierarchical variant of DBSCAN [3] to produce more refined clusters, which can help the domain expert to find and analyze these scenarios in more detail and investigate if we need to expand our scenario catalog with more new scenario classes or keep merging those sub-clusters into a larger scenario class.

We note that t-SNE was originally developed for visualisation and it may sometimes produce misleading results [40]. However, there are cases that t-SNE produces a satisfactory embedding for clustering [28] as in our case.

In Fig. 14b, we apply PCA with four principal components (that cover 75% of variance) and then apply the clustering method. As it is impossible to plot results in four dimensions, a two-dimensional representation of the trajectories obtained from t-SNE is used to plot the results. While K-means does not produce meaningful results in this four-dimensional space (we assume there is no spherical distribution expected by K-means), more reasonable results are achieved when applying DBSCAN instead. This can be seen in Fig. 14b, where four clusters are found. DBSCAN can extract complex and elongated clusters via establishing transitive relations, similar to minimax distance measures [16, 17] used in [19]. It is important to note that some points shown in red are labeled as noise.

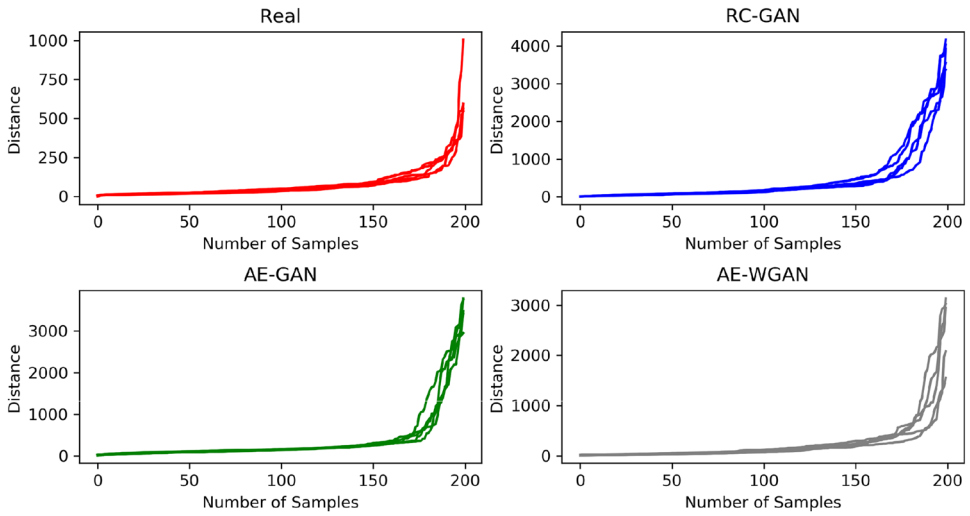

Fig. 12 The pairwise distances between matched samples in one-to-one matching: real: Red, RC-GAN: blue, AE-GAN: green, AE-WGAN: grey

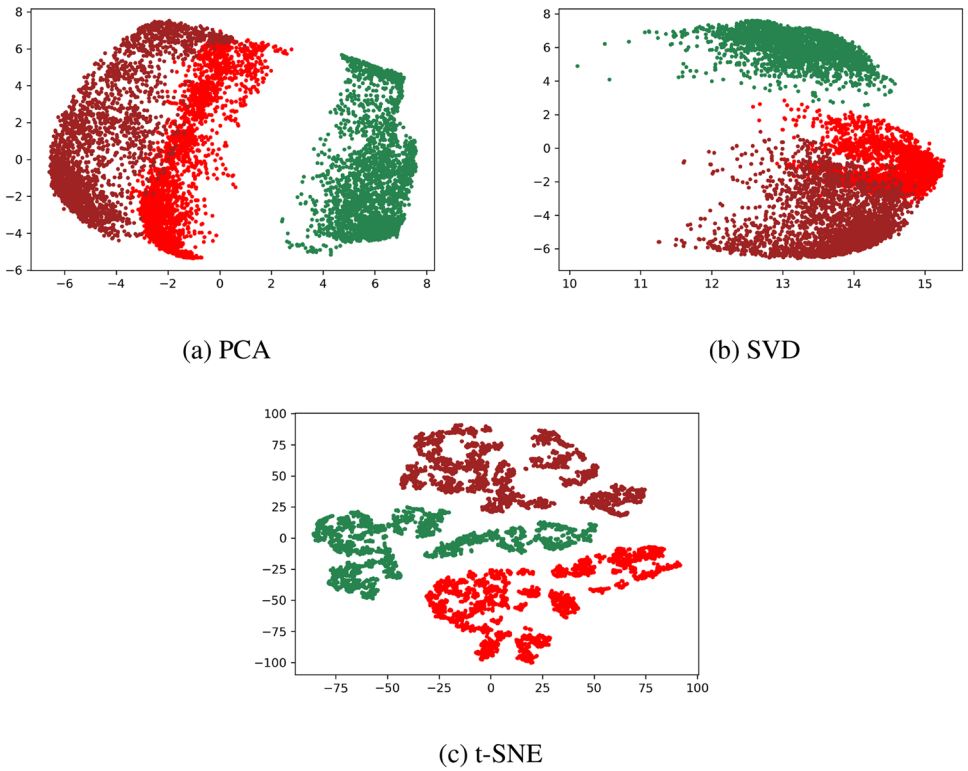

(a) PCA (b) SVD

(c) t-SNE

Fig. 13 Latent space representation of trajectories in two dimensions with ground-truth labels. green: right drive by, purple: left, red: cut-in

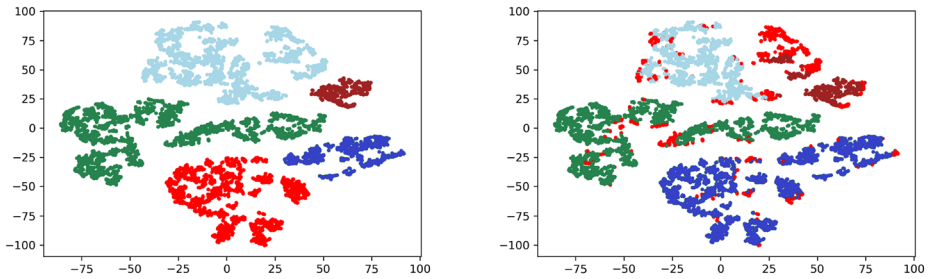

(a) DBSCAN applied to t-SNE embedding (b) DBSCAN applied to PCA (number of components=4). Red labels indicate noise.

Fig. 14 Results of DBSCAN on t-SNE embedding (**a**) and on PCA embedding (**b**). In (**b**) the visualization is based on t-SNE, but the labels are obtained by applying DBSCAN on PCA clustering

Processing and Detection of Outliers

Finally, we investigate the use of large reconstruction loss in autoencoder to detect anomalies of trajectories. Figure 15 illustrates the trajectories with high reconstruction loss within the studied set of 2000 cut-ins, say by having a threshold for max reconstruction (relative) error, as discussed in the previous section. We observe that most of the anomaly detected cut-ins are from decelerated cut-ins, which are a minority group w.r.t. all of the 2000 investigated cut-ins. Also, most of the anomalies (around one percent of the whole set with a high probability to be an outlier) are due to high jumps in the relative longitudinal distance between the ego and the detected surrounding car. This, in general, could be due to various reasons: anomalies in sensing reads of the surrounding object, sudden changes of the two drivers at the same time that can cause considerable changes in the measured relative distance, etc. Note that some jumps in longitudinal/lateral reads could be due to switching of the detected side of the surrounding cars, detected by the ego car sensor systems. Sensors calculate the relative distance based on the distance of the ego to the mid-point of the closest side of the adjacent cars. However, this side could switch when a car passes the ego car which leads to some jumps in the sensor readings.

A combination of different reasons could also be the root cause. Outlier detection can provide valuable information, even if we cannot precisely pinpoint the cause. It can be used to improve the quality of the original trajectory dataset,

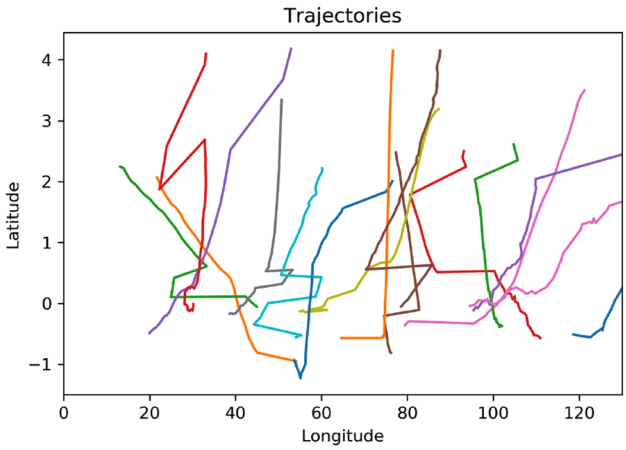

Fig. 15 Trajectories with a high probability of being an outlier, obtained by analysis of the autoencoder reconstruction loss

after some more detailed investigations of these anomalies are performed.

Conclusion

We developed a generic framework for generation and analysis of driving scenario trajectories based on modern deep neural network models. For trajectory generation, we studied the two generative models AE-GAN (with AE-WGAN-GP extension) and RC-GAN. We adapted them adequately to handle trajectories with variable length via proper batching the trajectories and integrating a neural component to learn the trajectory lengths. We also studied in detail the evaluation of the generated trajectories and elaborated several metrics accordingly.

In the following, we studied exploratory analysis of the latent representation from the recurrent autoencoder in a consistent way. In particular, we studied clustering and outlier detection mechanisms based the output of the trained recurrent autoencoder, where both of them demonstrate promising results.

The proposed framework can be extended in various ways as future work. (i) One direction could be a more sophisticated adjustment of the hyperparameters of the proposed models with more elegant techniques, rather than the simple grid search used in this work. (ii) AE-GAN is not a conditional model. Hence, to train the length estimator, we collected ground-truth labels for the length of each encoded trajectory. Then, these labels can be used as a condition to train a similar conditional model. (iii) Considering more features apart from only lateral and longitudinal positions could be possibly helpful for more complex scenarios.

Acknowledgements The work of Morteza Haghir Chehreghani was partially supported by the Wallenberg AI, Autonomous Systems and Software Program (WASP) funded by the Knut and Alice Wallenberg Foundation. We would like to acknowledge Volvo Cars for providing the data and the computational resources. We thank Viktor Wänerlöv and Rune Suhr from Volvo Cars, Scenario Analysis team, who helped us throughout the project.

Author Contributions The authors have contributed equally to this work. They have been involved in different steps.

Funding Open access funding provided by Chalmers University of Technology. The work of Morteza Haghir Chehreghani was partially supported by the Wallenberg AI, Autonomous Systems and Software Program (WASP) funded by the Knut and Alice Wallenberg Foundation.

Data Availability Statement The data are produced by Volvo Cars and does not contain any sensitive information, and all the personal information have been removed.

Declarations

Conflict of interest Not Applicable. No conflict of interest occurs.

Ethical approval This research is mainly focused on conceptual and methodological developments and the experimental studies use the datasets which do not contain any private and sensitive information.

Consent to participate Not applicable. There is no human study in this research.

Consent for publication Not applicable. No human study is performed in this research. There is no sensitive information.

Code availability The code will be available through the author's home page and will be maintained there with a reference to this publication.

References

1. Arnelid H, Zec EL, Mohammadiha N. Recurrent conditional generative adversarial networks for autonomous driving sensor modelling. In 2019 IEEE Intelligent Transportation Systems Conference (ITSC), IEEE, 2019, pp 1613–8.
2. Chehreghani MH. Adaptive trajectory analysis of replicator dynamics for data clustering. Mach Learn. 2016;104(2–3):271–89.

3. Chehreghani MH, Abolhassani H, Chehreghani MH. Improving density-based methods for hierarchical clustering of web pages. Data Knowl Eng. 2008;67(1):30–50.
4. Chehreghani MH, Rahgozar M, Lucas C, Chehreghani MH. A heuristic algorithm for clustering rooted ordered trees. Intell Data Anal. 2007;11(4):355–76.
5. Cho K, Van Merriënboer B, Gulcehre C, Bahdanau D, Bougares F, Schwenk H, Bengio Y. Learning phrase representations using rnn encoder-decoder for statistical machine translation. 2014. arXiv preprint arXiv:1406.1078
6. de Masson d'Autume C, Mohamed S, Rosca M, Rae J. Training language Gans from scratch. Adv Neural Inf Process Syst. 2019;32:4300–11.
7. Demetriou A, Allsvåg H, Rahrovani S, Chehreghani MH. Generation of driving scenario trajectories with generative adversarial networks. In: 23rd IEEE International Conference on Intelligent Transportation Systems, ITSC, 2020, pp. 1–6.
8. Ding W, Wang W, Zhao D. A new multi-vehicle trajectory generator to simulate vehicle-to-vehicle encounters. 2018. arXiv preprint arXiv:1809.05680
9. Donahue D, Rumshisky A. Adversarial text generation without reinforcement learning. 2018. arXiv preprint arXiv:1810.06640
10. Esteban C, Hyland SL, Rätsch G. Real-valued (medical) time series generation with recurrent conditional gans. 2017. arXiv preprint arXiv:1706.02633
11. Ester M, Kriegel H-P, Sander J, Xu X, et al. A density-based algorithm for discovering clusters in large spatial databases with noise. Kdd. 1996;96:226–31.
12. Gold O, Sharir M. Dynamic time warping and geometric edit distance: breaking the quadratic barrier. ACM Trans Algorithms. 2018;14(4):1–17.
13. Goodfellow I, Pouget-Abadie J, Mirza M, Xu B, Warde-Farley D, Ozair S, Courville A, Bengio Y. Generative adversarial nets. In: Advances in neural information processing systems. Cham: Springer; 2014. p. 2672–80.
14. Gulrajani I, Ahmed F, Arjovsky M, Dumoulin V, Courville AC. Improved training of wasserstein gans. In: Advances in neural information processing systems 30 (NIPS). Cham: Springer; 2017. p. 5767–77.
15. Haghir CM. Classification with minimax distance measures. In: Thirty-First AAAI Conference on Artificial Intelligence (AAAI), 2017, pp. 1784–90.
16. Haghir CM. Efficient computation of pairwise minimax distance measures. In: 2017 IEEE International Conference on Data Mining (ICDM), 2017, pp. 799–804.
17. Haghir CM. Unsupervised representation learning with minimax distance measures. Mach Learn. 2020;109(11):2063–97.
18. He K, Zhang X, Ren S, Sun J. Deep residual learning for image recognition. In: Proceedings of the IEEE conference on computer vision and pattern recognition, 2016, pp. 770–8.
19. Hoseini FS, Rahrovani S, Chehreghani MH. Vehicle motion trajectories clustering via embedding transitive relations. In: 24th IEEE International Intelligent Transportation Systems Conference, ITSC, IEEE, 2021, pp. 1314–21.
20. Hwang U, Jung D, Yoon S. Hexagan: generative adversarial nets for real world classification. In: Chaudhuri K, Salakhutdinov R, editors. International conference on machine learning, vol. 97. London: ICML; 2019. p. 2921–30.
21. Kalra N, Paddock SM. Driving to safety: how many miles of driving would it take to demonstrate autonomous vehicle reliability? Transp Res Part A. 2016;94:182–93.
22. Kim B, Kashiba Y, Dai S, Shiraishi S. Testing autonomous vehicle software in the virtual prototyping environment. IEEE Embed Syst Lett. 2016;9(1):5–8.
23. Kniaz VV, Knyaz V, Remondino F. The point where reality meets fantasy: mixed adversarial generators for image splice detection. In: Advances in neural information processing systems. Cham: Springer; 2019.
24. Krajewski R, Moers T, Nerger D, Eckstein L. Data-driven maneuver modeling using generative adversarial networks and variational autoencoders for safety validation of highly automated vehicles. In: 2018 21st International Conference on Intelligent Transportation Systems (ITSC), IEEE, pp. 2383–90.
25. Kurach K, Lucic M, Zhai X, Michalski M, Gelly S. A large-scale study on regularization and normalization in gans. In: Chaudhuri K, Salakhutdinov R, editors. International conference on machine learning. London: ICML; 2019. p. 3581–90.
26. Li X, Hu W, Hu W. A coarse-to-fine strategy for vehicle motion trajectory clustering. Int Conf Pattern Recognit. 2006;1:591–4.
27. Liao TW. Clustering of time series data-a survey. Pattern Recogn. 2005;38(11):1857–74.
28. Linderman GC, Steinerberger S. Clustering with t-sne, provably. SIAM J Math Data Sci. 2019;1(2):313–32.
29. Liu S, Zheng K, Zhao L, Fan P. A driving intention prediction method based on hidden markov model for autonomous driving. 2019. arXiv preprint arXiv:1902.09068
30. Lucic M, Kurach K, Michalski M, Gelly S, Bousquet O. Are gans created equal? A large-scale study. In: Advances in neural information processing systems. Cham: Springer; 2018. p. 700–9.
31. Maaten LVD, Hinton G. Visualizing data using t-sne. J Mach Learn Res. 2008;9:2579–605.
32. Malhotra P, Tv V, Vig L, Agarwal P, Shroff G. Timenet: pretrained deep recurrent neural network for time series classification. 2017. arXiv preprint arXiv:1706.08838
33. Martinsson J, Mohammadiha N, Schliep A. Clustering vehicle maneuver trajectories using mixtures of hidden markov models. In: 2018 21st International Conference on Intelligent Transportation Systems (ITSC), IEEE, 2018, pp. 3698–705.
34. Mogren O. C-rnn-gan: Continuous recurrent neural networks with adversarial training. 2016. arXiv preprint arXiv:1611.09904
35. Nguyen M, Purushotham S, To H, Shahabi C. m-tsne: A framework for visualizing high-dimensional multivariate time series. 2017. arXiv preprint arXiv:1708.07942
36. Takano W, A. Matsushita, K. Iwao, and Y. Nakamura. Recognition of human driving behaviors based on stochastic symbolization of time series signal. In: 2008 IEEE/RSJ International Conference on Intelligent Robots and Systems, IEEE, 2008, pp. 167–72.
37. Wang W, Ramesh A, Zhu J, Li J, Zhao D. Clustering driving encounter scenarios using connected vehicle trajectories. IEEE Trans Intell Veh. 2020;5:485–96.
38. Wang W, Zhao D. Extracting traffic primitives directly from naturalistically logged data for self-driving applications. IEEE Robot Autom Lett. 2018;3(2):1223–9.
39. Wang W, Zhao D. Extracting traffic primitives directly from naturalistically logged data for self-driving applications. IEEE Robot Autom Lett. 2018;3(2):1223–9.
40. Wattenberg M, Viégas F, Johnson I. How to use t-sne effectively. Distill. 2016.
41. Zhang H, Xu T, Li H, Zhang S, Wang X, Huang X, Metaxas DN. Stackgan++: realistic image synthesis with stacked generative adversarial networks. IEEE Trans Pattern Anal Mach Intell. 2019;41(8):1947–62.
42. Zhao D, Guo Y, Jia YJ. Trafficnet: An open naturalistic driving scenario library. In: 2017 IEEE 20th International Conference on Intelligent Transportation Systems (ITSC), IEEE, 2017, pp. 1–8.